STATISTICS, OPTIMIZATION AND INFORMATION COMPUTING
Stat., Optim. Inf. Comput., Vol. 11, January 2023, pp 125–135.
Published online in International Academic Press (www.IAPress.org)

Analysis of The Progressive Damage of A Notched AS4/PEEK Composite Laminate Subjected To Tensile Loading

Hamza El idrissi , Abbass Seddouki

Mechanical Engineering Laboratory, Faculty of Sciences and Techniques, Sidi Mohammed Ben Abdellah University, B.P. 2202 – Route d'Imouzzer, Fez, Morocco

Abstract The purpose of this work aims to assess the failure of an open-hole composite laminate subjected to tensile loading, using different progressive damage approaches. Within Abaqus, a user-defined material subroutine (UMAT) was developed and implemented by applying a combination of Puck's failure criterion and the gradual degradation model. In addition, the integrated model in Abaqus based on the Hashin failure criteria coupled with the continuous damage model has been also considered. Moreover, the effect of different specimen sizes on the behaviour of the AS4/PEEK composite laminate has been performed. The predicted results were compared to those available in the literature. The results of this comparative study showed good agreement between the experimental outcomes and the numerical predictions.

Keywords Progressive damage, Composite laminate, Failure criteria, Gradual stiffness degradation method, Finite element method

DOI: 10.19139/soic-2310-5070-1555

1. Introduction

Composite materials are commonly used in the aerospace sector owing to their great specific stiffness and strength, low weight and their suitability for various engineering designs. Furthermore, a large quantity of costly and time-consuming testing is required to ensure structural protection. More efficient failure theories and damage propagation models are considered essential to correctly predict failure processes in composite structures numerically and analytically, to solve this issue. Consequently, it is required to be able to evaluate the impact of parameters that can cause severe problems, including such geometrical discontinuities like holes, which can induce stress concentration in the structural analysis. The ply by ply reduction method of material degradation and continuous damage mechanics (CDM) models containing internal state variables are the two main types of failure propagation models.

However, several works have been carried out to analyse the damage of composite structures utilizing progressive failure analysis (PFA) methodologies based on damage mechanics and failure criteria [1, 2, 3, 4, 5, 6, 7]. Matzenmiller's approach coupled with Hashin's failure criteria is being employed today as a specific tool of the PFA [8]. Kweon et. al used a 2D finite element model which is based on damage progressive coupled with several classic failure criteria considering the stiffness degradation to assess the strength of the pinned joint [9].

The aim of this paper is to develop a finite element model, integrating the puck failure criteria coupled with the constant stress exposure (CSE), to forecast accurately the mechanical behaviour and progressive

*Correspondence to: Hamza El idrissi (hamza.elidrissi4@usmba.ac.ma). Mechanical Engineering Laboratory, Faculty of Sciences and Techniques, Sidi Mohammed Ben Abdellah University, B.P. 2202 – Route d'Imouzzer, Fez, Morocco.

ISSN 2310-5070 (online) ISSN 2311-004X (print)

damage of composite laminated, and also minimise calculation time and costs and to fully exploit the benefit of composite structures. Also, the built-in Abaqus model based on Hashin failure criteria coupled with Matzenmiller's approach was considered [10, 11]. As a result, the applied models allow us to estimate the AS4/PEEK open-hole composite laminates' failure load and progressive damage.

2. Overview of theories for the initial/progressive of intralaminar damage

2.1. Introduction

Matrix cracking, fiber breakage and inter-layer delamination are the prevalent damage mechanisms in composite laminates. Furthermore, the different damage mechanism that occur in both the matrix and the fiber can be classified as intralaminar damage, whereas delamination is classified as interlaminar damage. In this paper, only intralaminar damage has been taken into account in the applied composite damage model, which has been incorporated as a UMAT subroutine within the Abaqus software.

2.2. Intralaminar damage initiation

In case of intralaminar damage, due to the inhomogeneous nature of the composite materials, several failure mechanisms can be observed under different loads. Hashin has introduced four independent equations that differentiated into tension and compression parts, related to four different damage initiation mechanisms that are much more complex in its application, in contrast to conventional failure criteria that ignore the interaction between damage mechanism such as the Tsai-Hill and maximum stress/strain criteria.

Besides, Puck and Schurmann have gained the confidence of the community by following the Hashin criterion strategy, which is physically based on appropriate assumptions and mathematical formulations for brittle fracture [10, 11]. Their theory has become very reliable in terms of damage prediction for the following reasons; fiber failure (FF) is related to the properties of the fiber instead of the properties of the layer, inter-fiber failure (IFF) has been differentiated into three mechanisms (A, B, C) which depend on the nature of the applied load and the most important is the proposed procedure for determining the fracture plane angle arising from the damage of composite laminated. As a consequence, the Puck failure criterion is defined as follows.

Fiber failure (FF):

$$F_{E,(FF)} = \frac{\sigma_{11} - (\nu_{\perp\parallel} - \nu_{\perp\parallel f} m_{\sigma f} \frac{E_{\parallel}}{E_{\parallel f}})(\sigma_{22} + \sigma_{33)}}{\pm R_{\parallel}^{t,c}} \tag{1}$$

$$with \begin{cases} +R_{\parallel}^{t} : \ for\ tension \\ -R_{\parallel}^{c} : \ for\ compression \end{cases}$$

$F_{E,FF}$ is the failure index related to the fiber, $\pm R_{\parallel}^{t,c}$ represent the tensile and compressive strengths of the composite laminated. σ_{11}, σ_{22} and σ_{33} are the normal stresses acting in the lamina, $\nu_{\perp\parallel}$ and $\nu_{\perp\parallel f}$ are the Poisson's ratio related to lamina and fibers, respectively. $E_{\parallel}$ and $E_{\parallel f}$ correspond to the longitudinal modulus of the lamina and the fibers, respectively and $m_{\sigma f}$ denote the transverse stress amplification factor in the fibers.

For a pure tensile load, this criterion behaves like the criterion of the maximum stress. However, the effect is more noticeable under higher transverse stresses. Fiber failure according to Puck's theory is the last failure of the laminate ply.

Inter-fiber failure (IFF):

The criteria for failure of the action plan are formulated by means of the following stresses σ_n,τ_{nt} and τ_{n1} instead of σ_{11}, σ_{22}, σ_{33}, τ_{12}, τ_{13} and τ_{23} that are located on a parallel plane towards the fibers and at

an angle θ. However, these stresses are obtained by applying the transformations below:

$$\begin{pmatrix}\sigma_n(\theta)\\ \tau_{nt}(\theta)\\ \tau_{n1}(\theta)\end{pmatrix} = \begin{pmatrix} C^2 & S^2 & 2SC & 0 & 0\\ -CS & CS & (C^2-S^2) & 0 & 0\\ 0 & 0 & 0 & S & C\end{pmatrix}\begin{pmatrix}\sigma_{22}\\ \sigma_{33}\\ \tau_{23}\\ \tau_{13}\\ \tau_{12}\end{pmatrix} \tag{2}$$

Where $C = \cos\theta$ and $S = \sin\theta$
For $\sigma_n \geq 0$

$$F_{E_{(IFF)}}(\theta) = \sqrt{[(\frac{1}{R_{\perp}^{At}} - \frac{p_{\perp\psi}^{t}}{R_{\perp\psi}^{A}})\sigma_n(\theta)]^2 + (\frac{\tau_{nt}(\theta)}{R_{\perp\perp}^{A}})^2 + (\frac{\tau_{n1}(\theta)}{R_{\perp\parallel}^{A}})^2} + \frac{p_{\perp\psi}^{c}}{R_{\perp\psi}^{A}}\sigma_n(\theta) \tag{3}$$

For $\sigma_n < 0$

$$F_{E_{(IFF)}}(\theta) = \sqrt{[\frac{p_{\perp\psi}^{c}}{R_{\perp\psi}^{A}})\sigma_n(\theta)]^2 + (\frac{\tau_{nt}(\theta)}{R_{\perp\perp}^{A}})^2 + (\frac{\tau_{n1}(\theta)}{R_{\perp\parallel}^{A}})^2} + \frac{p_{\perp\psi}^{t}}{R_{\perp\psi}^{A}}\sigma_n(\theta) \tag{4}$$

Where
$\frac{p_{\perp\psi}^{t,c}}{R_{\perp\psi}^{A}} = \frac{p_{\perp\perp}^{t,c}}{R_{\perp\perp}^{A}}\cos(\psi)^2 + \frac{p_{\perp\parallel}^{t,c}}{R_{\perp\parallel}^{A}}\sin(\psi)^2$
$\cos(\psi)^2 = 1 - \sin(\psi)^2 = \frac{\tau_{nt}^2}{\tau_{nt}^2 - \tau_{n1}^2}$

$R_{\perp\parallel}^{A} = \frac{R_{\perp}^{c}}{2(1+p_{\perp\perp}^{c})}$

$R_{\perp\parallel}^{A}$ and $R_{\perp}^{At}$ indicate the in-plane shear strength and the tensile strength perpendicular through the fiber direction, respectively. $R_{\perp\parallel}^{A}$ is the fracture resistance caused by transverse/transverse shear stress. θ_{fp} indicates the fracture plane angle. $F_{E_{(IFF)}}$ is the failure index related to the inter-fiber of the lamina. furthermore, when the value of $f_E = 1$ is reached, it is termed as the fracture condition of the lamina. Moreover, if σ_n corresponds to a tensile stress, it favours the inter-fiber failure by supporting shear stresses. However, if σ_n corresponds to a compressive stress, it would restrain the inter-fiber failure by enhancing the resistances to fracture through shear fractures. Consequently, distinct equations are employed to predict inter-fiber failure in tension and compression σ_n as outlined above. $p_{\perp\perp}^{t,c}$ and $p_{\perp\parallel}^{t,c}$ are the inclination parameters and obtained from the (σ_{22}, τ_{12}) curves. Puck has provided recommended values for these slope parameters, as shown below in Table 1. However, it is difficult to obtain these parameters without doing a series of experiments.

Table 1.
Recommended values for inclination parameters

Laminate	$p_{\perp\parallel}^{c}$	$p_{\perp\parallel}^{t}$	$p_{\perp\perp}^{t,c}$
Glass fiber-reinforced polymer	0.25	0.30	0.20-0.25
Carbon fiber-reinforced polymer	0.30	0.35	0.25-0.30

2.3. Intralaminar damage evolution

The appropriate approach must be applied to assess the growth of damage to final failure, in the same manner as the damage identified in the composite material. The method used in this work is the constant stress exposure (CSE), which is a gradual stiffness degradation method [12]. Moreover, the degradation process is supposed to be the growth of crack density. Furthermore, it should be mentioned that the effect

of delamination on the mechanical response of composite laminates with embedded plies is very negligible under in-plane loading , thus, the applied approach used in this work ignores the delamination failure.

Concerning phenomenology of damage, the onset and propagation of defects in a material are highly dependent on the gradual degradation of its performance, the highlight of which is the decline in the rigidity of the substance. Furthermore, The progressive damage of a composite laminated can be quantified, using the relationship between the accumulation of internal material damage and the decrease in material stiffness, including a theoretical and numerical approach.

Once the stress exposure reaches a value of one, the selected elastic properties of elements are reduced to zero in compliance with equations for the inter-fiber failure, the modulus perpendicular to fibers and in-plane shear modulus are degraded. However, in the case of fiber failure, all the elastic properties are reduced. Furthermore, The stiffness component of E_{ij} and G_{ij} are decrease in different ways [13].

The material is considered linearly elastic with transversely orthotropic material behaviour. The constitutive elastic stress/strain equations, the input parameters of the material for the prediction of the onset and progressive damage based on the (Puck-CSE) as well as the fiber/matrix damage variables can be stated in the following way. Also, the degradation rules used are listed below in Table 2:

$$\{\sigma\} = [C]\{\epsilon\} \tag{5}$$

$$\begin{pmatrix}\sigma_{11}\\ \sigma_{22}\\ \sigma_{33}\\ \sigma_{12}\\ \sigma_{13}\\ \sigma_{23}\end{pmatrix} = \begin{pmatrix}C_{11} & C_{12} & C_{13} & 0 & 0 & 0\\ C_{12} & C_{22} & C_{23} & 0 & 0 & 0\\ C_{13} & C_{23} & C_{33} & 0 & 0 & 0\\ 0 & 0 & 0 & 2G_{12}^{red} & 0 & 0\\ 0 & 0 & 0 & 0 & 2G_{13}^{red} & 0\\ 0 & 0 & 0 & 0 & 0 & G_{23}^{red}\end{pmatrix}\begin{pmatrix}\epsilon_{11}\\ \epsilon_{22}\\ \epsilon_{33}\\ \epsilon_{12}\\ \epsilon_{13}\\ \epsilon_{23}\end{pmatrix} \tag{6}$$

$$d_f = 1 - (1 - d_{ft})(1 - d_{fc}) \tag{7}$$

$$d_f = 1 - (1 - d_{ft})(1 - d_{fc}) \tag{8}$$

$$C_{11} = E_{11}^{red}(1 - \nu_{23}\nu_{32})\Delta \tag{9}$$

$$C_{22} = E_{22}^{red}(1 - \nu_{13}\nu_{31})\Delta \tag{10}$$

$$C_{33} = E_{33}^{red}(1 - \nu_{12}\nu_{21})\Delta \tag{11}$$

$$C_{12} = E_{11}^{red}(\nu_{21} - \nu_{31}\nu_{23})\Delta \tag{12}$$

$$C_{13} = E_{22}^{red}(\nu_{32} - \nu_{12}\nu_{31})\Delta \tag{13}$$

$$C_{23} = E_{33}^{red}(\nu_{31} - \nu_{21}\nu_{32})\Delta \tag{14}$$

$$\Delta = \frac{1}{1 - \nu_{12}\nu_{21} - \nu_{23}\nu_{32} - \nu_{13}\nu_{31} - 2\nu_{21}\nu_{32}\nu_{13}} \tag{15}$$

$$E_{11}^{red} = E_{11}^{orig}(1 - d_{ft})(1 - d_{fc}) \tag{16}$$

$$E_{22}^{red} = E_{22}^{orig}(1-d_{ft})(1-d_{fc})(1-d_{mt})(1-d_{mc}) \tag{17}$$

$$E_{33}^{red} = E_{22}^{red} \tag{18}$$

$$G_{12}^{red} = G_{12}^{orig}(1-d_{ft})(1-d_{fc})(1-kd_{mt})(1-kd_{mc}) \tag{19}$$

$$G_{13}^{red} = G_{12}^{red} \tag{20}$$

$$G_{23}^{red} = G_{23}^{orig}(1-d_{ft})(1-d_{fc})(1-kd_{mt})(1-kd_{mc}) \tag{21}$$

$$\nu_{21} = \frac{E_{22}^{red}}{E_{11}^{red}}\nu_{12} \tag{22}$$

$$\nu_{31} = \frac{E_{33}^{red}}{E_{11}^{red}}\nu_{13} \tag{23}$$

Table 2.
The requirements of each failure mechanism for (CSE)

Failure mechanisms	Requirement for validity	Damage value
Tensile fiber mechanism	$\sigma_{11} > 0$	$d_{ft} = 1$
Compressive fiber mechanism	$\sigma_{11} < 0$	$d_{fc} = 1$
Tensile matrix mechanism	$\sigma_n > 0$	$d_{mt} = 1$
Compressive matrix mechanism	$\sigma_n < 0$	$d_{mc} = 1$

3. Numerical analysis processes

3.1. Problem Description

The progressive damage of AS4/PEEK composite laminates, including stress concentration and charged by a tensile load in-plane, has been examined using numerical simulations. Furthermore, the material is supposed to be linearly elastic and transversely orthotropic. In addition, the analysis included the prediction of failure load and the load-displacement curves.

On the other hand, there are numerous numerical findings available in the literature as Chen et al, Mandal et al [14, 15] and the experimental data reported by Maa and Cheng [16] were chosen to compare and validate the proposed approaches. The dimensions, the properties and the geometry of the employed laminate are presented in Table3, Table 4 and Figure 1, respectively.

The virtual sample has been discretised with four-node linear-reduced integration (SC8R) quadrilateral elements using a size of (1mm×1mm) which was created in Abaqus 2017. However, the reason for choosing the continuous shell is that we have assumed a plane stress problem since we have applied in-plane loading and therefore out of plane stresses are neglected. The laminate has been subjected to the controlled load by displacement.

To simulate it, a linear constraint equation was employed at the loading surface with displacement-controlled loading being applied at a the reference point (RP) and is positioned at the end of the loading nose. The purpose of that is to ensure that the displacements would be uniform across all nodes on that loaded surface and the reference point (RP). As a result, surface displacement and reaction load at this reference node can be tracked. Due to the obvious problem's symmetry, we were able to simulate one-quarter of the model as shown in Figure 2. The composite laminates consist of eight layers of the same thickness with the following stacking sequences $[0/45/90/-45]_{2s}$.

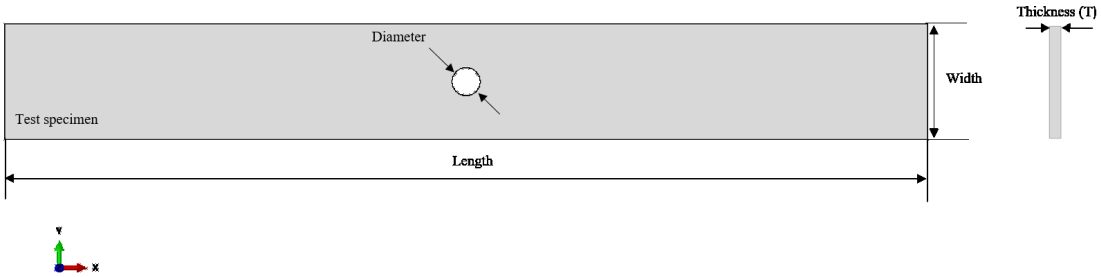

Figure 1. The geometry of the AS4/PEEK composite laminates

Table 3.
Dimensions of the specimen used in this study

	Length (mm)	Height (mm)	Thickness (mm)	Diameter (mm)
AS4/PEEK	100	20	2	2 5 10

Table 4.
Material properties of AS4/PEEK test specimen[14]

Properties	AS4/PEEK
$E_{11}(GPa)$	127.6
$E_{22}(GPa)$	10.3
$G_{12}(GPa)$	6.0
ν_{12}	0.32
ν_{23}	0.45
$X_T(MPa)$	2023.0
$X_C(MPa)$	1234.0
$Y_T(MPa)$	92.7
$Y_C(MPa)$	176.0
$S_{12}(MPa)$	82.6
$G_{1t,c}(N/mm)$	128.0
$G_{1c,c}(N/mm)$	128.0
$G_{2t,c}(N/mm)$	5.6
$G_{2c,c}(N/mm)$	9.31

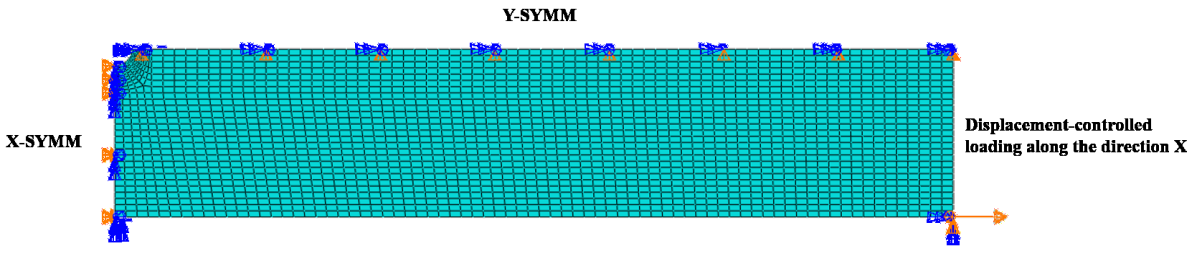

Figure 2. One-quarter of the finite element model

3.2. Failure Analysis Procedure Using Abaqus

To assess the onset failure of composite laminated subjected to tensile stress, the Hashin and Puck failure criteria were applied to each element. During the analysis, the stiffness matrix, strains, and stresses for each

element at each gauss point in the material are computed. Once the failure was identified using Equations

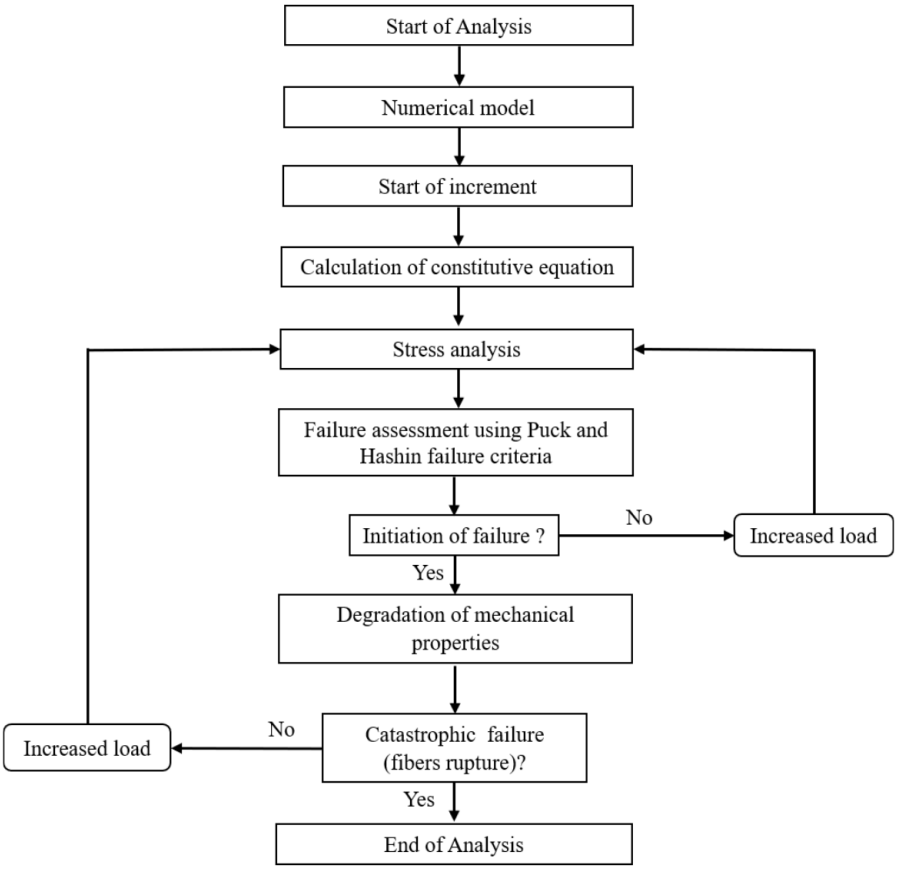

Figure 3. The computational algorithm

(1-4) , the failed element was deteriorated utilizing progressive failure theories following Equations (7-23), and the stresses and strains were calculated again by Equations (5-6) until the affected areas were completely failed. The algorithm of computation is presented in Figure 3.

4. Computational Analysis Results

The predicted results for an open-hole AS4/PEEK using numerical modelling are shown in Table 5.

Table 5.
The failure loads (KN) of AS4/PEEK composite laminates

Hole diameter	Chen et al	Mandal et al	Present model	Built-in model	Test
2	21.649	27.287	23.0033	15.0855	22.98
5	16.431	22.493	17.5565	12.2399	15.31
10	10.581	14.701	10.1929	7.68998	9.22

Various studies predict different failure load values, this is due to the many failure theories available which are not necessarily predict the same failed lamina and failure process. The built-in model in Abaqus

and the model present by Mandal et al [15] are insufficient to accurately estimate the failure load and have a significant error with the test result.

Firstly, these differences may be explained through the failure criteria considered to identify the occurrence of the damage, where they do not include the definition of the fracture plane angle. Secondly, the adjustment loss parameters for shear stiffness components induced by matrix failure in tension and compression, were overlooked in the stiffness discount strategy used by Mandal et al [15].

However, the present model shows strong compliance with the test data. Indeed, Puck's criteria are among the most precise in which Puck incorporated the fracture angle of the fracture plane and pointed out the need to take it into account. The progressive process used in the Present model offers the possibility of monitoring stiffness degradation where the stiffness characteristics of the lamina are reduced as the stress increases. Therefore, the residual stiffness of the lamina is taken into consideration, whereas the Matzenmiller method neglects this element. Likewise, the ultimate failure load is defined by the configuration type of the laminate under both the load and boundary conditions, as well as by the material and size of the composite laminate.

To better understand the damage process, Figures (4,5) show the onset and spread of damage using the applied models. As can be seen, the matrix starts failing in the layers with 90°orientation at the same load for both the Present model and the built-in model. the same for the initial fiber failure which occurred in the first layer that oriented at 0° with a low load of 6.96 KN. Because of the highest quantity of damage, the failure of the tensile fibers is seen to develop at the layer with an orientation of 0°. It may be stated that the presence of the 45° layers next to the 0° layer causes the formation of extreme shear stress in the plane, which has a significant impact on the Hashin and Puck equations for tensile fiber failure [17].

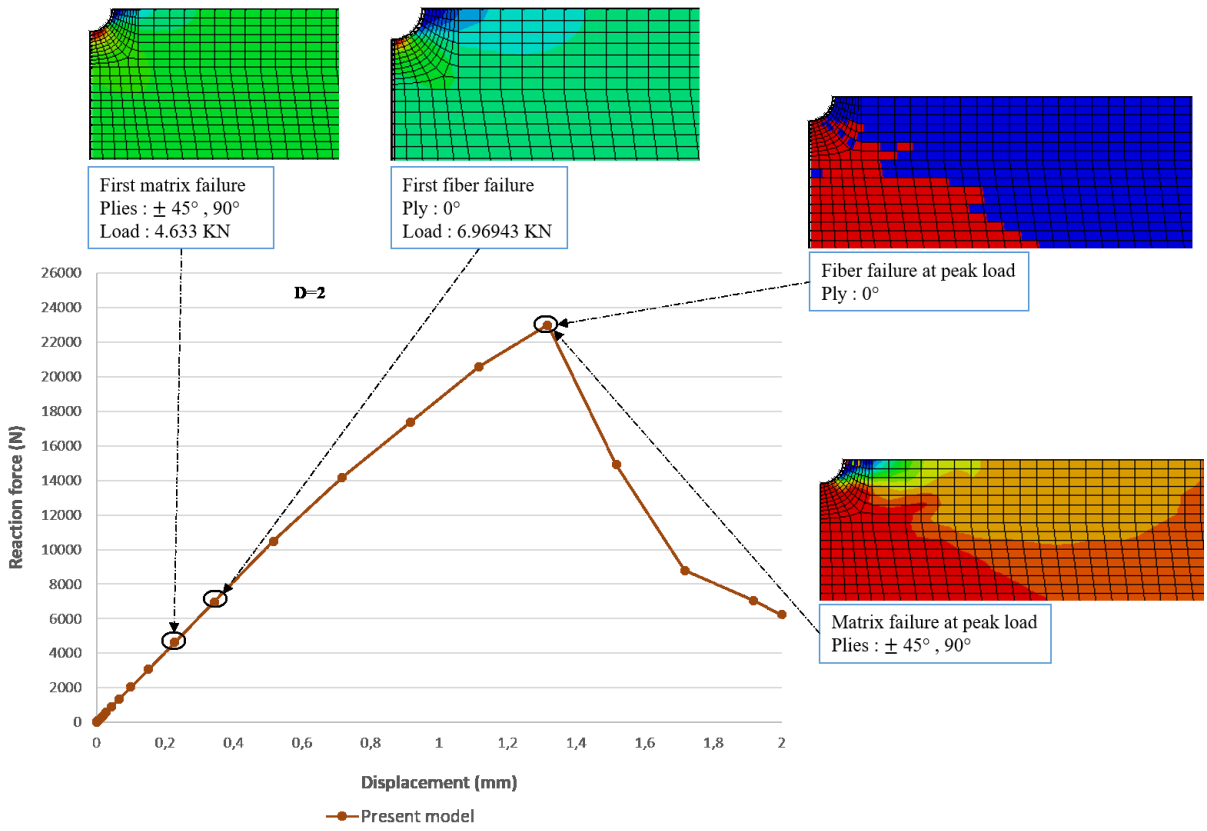

Figure 4. Load vs. displacement curve for the Present model

Catastrophic failure occurs throughout the layers due to a decrease in all material properties at the maximum tensile fiber failure load, which is 23.0033 KN for the Present model. Also, in parallel to the matrix failure mechanism, there is little damage to the 0° orientation plies, leading to insignificant loss to the 0° layers. The Built-in model has 15.0855 KN for the fiber tension failure mode at peak load, and the damage variable surpasses one after the ultimate load, making a total fracture of the composite laminated. The damage began at the edge of the open-hole since to the noticeable stress concentration. Furthermore, severe damage doesn't occur for failure fiber in layers with 90° orientation, whereas the damage variable of Matzenmiller's method simply lowers fiber stiffness in this failure mode.

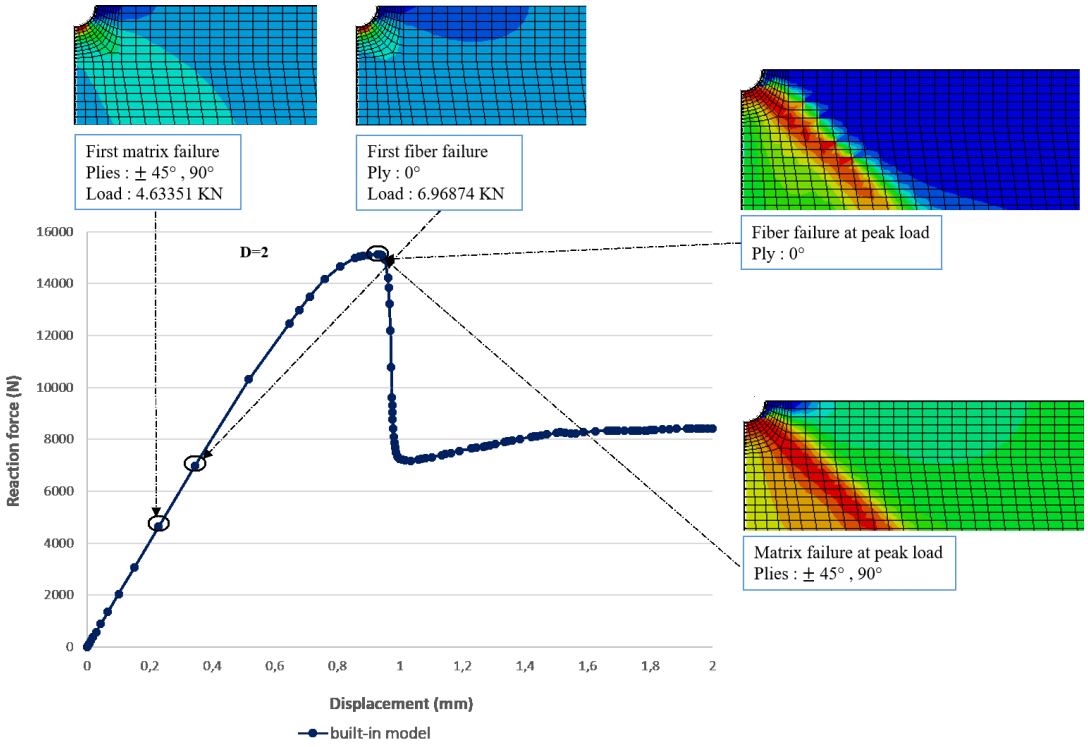

Figure 5. Load vs. displacement curve for the built-in model

Figure 6 displays the associated failure load predictions based on the Present model and the built-in Abaqus model, compared to the test values. In fact, the AS4/PEEK constituents were fabricated from the same laminate and have identical stiffness, the ultimate load of this laminate strongly depends on the specimen size. from this figure, it can be noticed that the predicted failure load and the experimental values decrease when the hole diameter increases. The analysis results of the effect of specimen size on the open-hole composite laminated were established by the Present model, and most of the predictions are within the confidence interval, in contrast to the integrated model which gives a higher error during the failure load analysis with different hole diameters.

5. Conclusion

In the present work, an open-hole AS4/PEEK composite laminate has been examined under tensile loading to quantify the damage process starting from the onset of damage until the final failure.

It was found that the behaviour of the AS4/PEEK, which was predicted using the progressive stiffness degradation approach coupled with Puck failure criteria, had been in substantial agreement

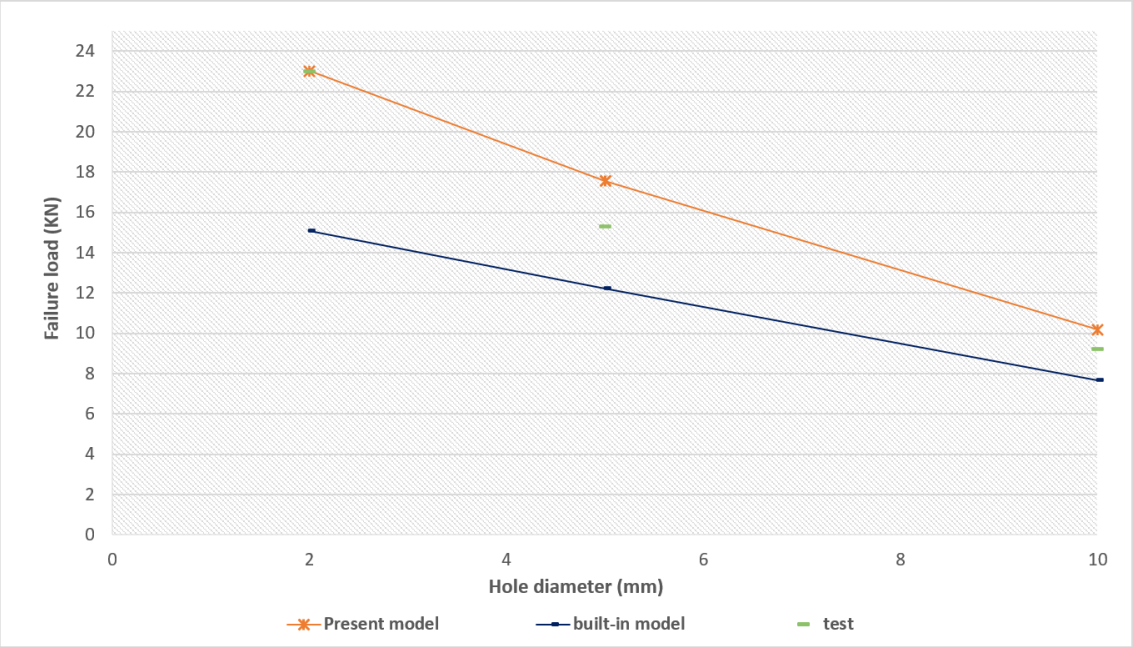

Figure 6. Relationships between failure load and different diameters

with experimental results given in the literature and became more accurate than the Abaqus built-in model. Aside from that, the actual model has the ability to precisely track the stiffness of the composite material and the influence of varied specimen sizes on the open-hole composite laminate. In addition, the structural failure analysis of large and complex composite structures may be possible. Needless to say, the analysis time is relatively higher because the Puck criteria require an iterative process of obtaining the fracture plan angle.

Acknowledgement

The authors would like to thank the editors and reviewers for their constructive comments and their helpful suggestions, which helped us to improve the quality of this paper in order to make it appropriate for publication .

REFERENCES

1. A. I. Khan, "Progressive failure analysis of laminated composite structures," Ph.D. dissertation, Virginia Tech, 2015.
2. D. Yoon, S. Kim, J. Kim, and Y. Doh, "Development and evaluation of crack band model implemented progressive failure analysis method for notched composite laminate," Applied Sciences, vol. 9, no. 24, p. 5572, 2019.
3. Z. C. Su, T. E. Tay, M. Ridha, and B. Chen, "Progressive damage modeling of open-hole composite laminates under compression," Composite Structures, vol. 122, pp. 507–517, 2015.
4. Y. Cao, Z. Cao, Y. Zhao, D. Zuo, and T. Tay, "Damage progression and failure of single-lap thin-ply laminated composite bolted joints under quasi-static loading," International Journal of Mechanical Sciences, vol. 170, p. 105360, 2020.
5. X. Li, D. Ma, H. Liu, W. Tan, X. Gong, C. Zhang, and Y. Li, "Assessment of failure criteria and damage evolution methods for composite laminates under low-velocity impact," Composite structures, vol. 207, pp. 727–739, 2019.
6. H. El idrissi and A. Seddouki, "Modelling of progressive damage in a notched carbon/epoxy composite laminate subjected to tensile loading using different assessment methods coupled with fem," Fibers and Polymers, pp. 1–17, 2022.

7. H. El Idrissi and A. Seddouki, "Damage modeling of composites laminate containing stress concentrations," in 2022 2nd International Conference on Innovative Research in Applied Science, Engineering and Technology (IRASET), 2022, pp. 1–5.
8. A. Matzenmiller, J. Lubliner, and R. L. Taylor, "A constitutive model for anisotropic damage in fiber-composites," Mechanics of materials, vol. 20, no. 2, pp. 125–152, 1995.
9. J.-H. Kweon, S.-Y. Shin, and J.-H. Choi, "A two-dimensional progressive failure analysis of pinned joints in unidirectional-fabric laminated composites," Journal of composite materials, vol. 41, no. 17, pp. 2083–2104, 2007.
10. Z. HASHIN, "Failure criteria for unidirectional composites," International Journal of Applied Mechanics and Engineering, vol. 47, pp. 329–334, 1980.
11. A. Puck and H. Schürmann, "Failure analysis of frp laminates by means of physically based phenomenological models," Composites science and technology, vol. 62, no. 12-13, pp. 1633–1662, 2002.
12. C. A. Coulomb, "Essai sur une application des regles de maximis et minimis a quelques problemes de statique relatifs a l'architecture (essay on maximums and minimums of rules to some static problems relating to architecture)," Mem. Div. Sav. Acad, vol. 7, 1973.
13. H. M. Deuschle, "3d failure analysis of ud fibre reinforced composites: Puck's theory within fea," Ph.D. dissertation, University of Stuttgar, 2010.
14. B. Chen, T. Tay, P. Baiz, and S. Pinho, "Numerical analysis of size effects on open-hole tensile composite laminates," Composites Part A: Applied Science and Manufacturing, vol. 47, pp. 52–62, 2013.
15. B. Mandal and A. Chakrabarti, "Simulating progressive damage of notched composite laminates with various lamination schemes," International Journal of Applied Mechanics and Engineering, vol. 22, no. 2, 2017.
16. R.-H. Maa and J.-H. Cheng, "A cdm-based failure model for predicting strength of notched composite laminates," Composites Part B: Engineering, vol. 33, no. 6, pp. 479–489, 2002.
17. H. Bakhshan, A. Afrouzian, H. Ahmadi, and M. Taghavimehr, "Progressive failure analysis of fiber-reinforced laminated composites containing a hole," International Journal of Damage Mechanics, vol. 27, no. 7, pp. 963–978, 2018.